

## Antiferromagnetism in 3d transition metals

V. L. Moruzzi and P. M. Marcus

*IBM Research Division, Thomas J. Watson Research Center, P.O. Box 218, Yorktown Heights, New York 10598*

(Received 23 March 1990)

Total-energy band calculations using the local-spin-density approximation, the augmented-spherical-wave method, and the fixed-spin-moment procedure are used to investigate the volume dependence of the magnetic and electronic properties of 3d transition metals constrained to cubic environments in one-atom or two-atom unit cells. The calculations cover a range of volumes spanning the nonmagnetic-ferromagnetic and the nonmagnetic-antiferromagnetic transitions. We find antiferromagnetism in bcc vanadium at expanded volumes, show that bcc chromium has a first-order transition from nonmagnetic to antiferromagnetic behavior at a 2% expanded lattice constant, and find that previously reported antiferromagnetic solutions for bcc iron are unstable. Comments are made on when antiferromagnetism occurs and on the many-atom ground states for chromium and manganese.

### I. INTRODUCTION

Although the volume dependence of transition-metal ferromagnetism is easily calculated using first-principles band theory,<sup>1-3</sup> the calculation of the volume dependence of antiferromagnetism is more subtle. Among the 3d transition metals, well-defined antiferromagnetic ground states occur only for chromium and manganese, although not in simple lattice structures. The known antiferromagnetic character of the ground state of these elements has led to a number of total-energy band calculations<sup>4-13</sup> that attempt to establish the existence and properties of that state. These calculations have generally involved simplifying constraints and unrealistic magnetic unit cells. Such calculations have also been reported on bcc and fcc iron.<sup>11,14,15</sup> However, the stability of these various calculated antiferromagnetic states against more complex spin arrangements or lattice distortions<sup>9,13</sup> has not been adequately explored. We give examples of the occurrence of instabilities in this work.

Total-energy band calculations for an antiferromagnetic elemental system with cubic symmetry essentially require a spin-polarized calculation with at least a two-atom magnetic unit cell such as a CsCl-type for the bcc case and a CuAu-type for the fcc case. The two atoms are conventionally constrained to have equal and opposite local moments (thus excluding ferromagnetic and ferrimagnetic solutions), but the magnitude of the local moments is allowed to vary so as to minimize the total energy in a self-consistent scheme. The system is then considered to be antiferromagnetic or nonmagnetic according to whether the magnitude of the local moment is found to be finite or zero. In the present work we use a different and more flexible constraint that finds ferromagnetic and ferrimagnetic as well as antiferromagnetic states.

Recently, we have applied a spin-polarized fixed-spin-moment procedure<sup>16</sup> to ferromagnetic states using one-atom cells to determine the total-energy  $E$  as a function of constrained magnetic moment  $M$  for different volumes

$V$ . The minima in calculated  $E(M)_V$  curves, which correspond to zero-magnetic-field solutions, give the volume dependence of the magnetic behavior of the system. A minimum of  $M=0$  in a calculated energy versus moment curve signifies a nonmagnetic state. A maximum at  $M=0$  and a minimum at a finite  $M$  value implies an unstable nonmagnetic state and a stable ferromagnetic state with a moment indicated by the minimum. Using this procedure, we have shown<sup>2,3</sup> that all transition metals undergo a transition from nonmagnetic to ferromagnetic behavior with increasing volume. These magnetovolume transitions are generally second order for early and late transition metals, but are first order or complicated mixtures of second order and first order for midtransition metals. Note that conventional band calculations (without fixed-spin-moment capabilities) have generally not given an accurate description of these magnetovolume transitions; they usually show gradual and continuous increases in magnetic moment as the volume increases rather than the sharp (sometimes discontinuous) transitions found by our fixed-spin-moment procedure.

A straightforward generalization of our fixed-spin-moment procedure to two-atom magnetic unit cells permits the study of antiferromagnetic and ferrimagnetic as well as ferromagnetic and nonmagnetic states. In this generalization, the total moment  $M$  is fixed but the local moments  $m_a$  and  $m_b$  of the two inequivalent atoms (with the same atomic number) are allowed to vary so as to minimize the total energy in a self-consistent iteration scheme.<sup>17</sup> For  $M=0$ , the system can now assume either a nonmagnetic or an antiferromagnetic state. A minimum at  $M=0$  implies stability with respect to variation of  $M$ , while a local maximum implies instability. Thus, analysis of calculated  $E(M)$  curves permits determination of multiple stable (and metastable) solutions at a given volume. Using these procedures we have shown<sup>11</sup> the existence of antiferromagnetic states in both manganese and iron constrained to an fcc (CuAu) lattice. In addition, we have found evidence<sup>12</sup> for stable ferrimagnetic and antiferromagnetic states in bcc (CsCl) manganese. We find that

stable antiferromagnetic (or ferrimagnetic) states seem to occur only for systems that exhibit first-order or mixed transitions when studied with a one-atom unit cell (fcc or bcc) constraint. The gradual change represented by a second-order transition is apparently energetically more favored than the abrupt change represented by a first-order transition. This observation of the occurrence of antiferromagnetism when first-order ferromagnetic transitions occur provided the motivation to study antiferromagnetism in CsCl-type vanadium, chromium, and iron. We have already shown that bcc vanadium<sup>2,3</sup> and chromium<sup>2</sup> exhibit mixed or first-order nonmagnetic to ferromagnetic transitions, and that bcc iron<sup>2</sup> exhibits a second-order transition.

## II. RESULTS

All of our results are based on the augmented-spherical-wave method by Williams, Kübler, and Gelatt,<sup>18</sup> which assumes a sphericalized potential within Wigner-Seitz spheres of radius  $r_{WS}$ . We use the local-spin-density approximation as formulated by von Barth and Hedin and modified by Janak<sup>19</sup> to account for exchange and correlation. All calculations are nonrelativistic, utilize the fixed-spin-moment procedure,<sup>16</sup> and are done on a uniform mesh of 84 points in the irreducible  $k$ -space wedge of the Brillouin zone of the two-atom cell.

### A. Vanadium

Previous total-energy band calculations on bcc vanadium<sup>2,3,20</sup> were done only for a one-atom per unit cell system, and therefore did not consider possible antiferromagnetic solutions. In Fig. 1 we show the results of a two-atom per unit cell CsCl fixed-spin-moment calculation. We note that the equilibrium state is nonmagnetic at  $r_{WS} \approx 2.78$  a.u. and that the antiferromagnetic state is energetically more favored than the nonmagnetic (NM), the low-spin<sup>2</sup> (LS), or the ferromagnetic (FM) state at expanded volumes, in agreement with the above observation. In fact, the transition from the nonmagnetic state to the preferred antiferromagnetic state is second order as shown on an expanded scale in Fig. 2 by the gradual merging of the low spin and antiferromagnetic total-energy curves and the continuous increase in the local antiferromagnetic moments from zero to values approaching the ferromagnetic moments for volumes above the transition. This second-order transition occurs at  $r_{WS} \approx 3.15$  a.u., just below  $r_{WS} \approx 3.24$ , where we find a one-atom per unit-cell transition from the nonmagnetic to the ferromagnetic (low-spin) state.

### B. Chromium

Total-energy band calculations for chromium generally simplify the model of the antiferromagnetic state by noting that the incommensurate spin-density wave found experimentally is close to a bcc lattice with CsCl magnetic structure. Previous work<sup>5,7,8,10</sup> has not, however, given an accurate description of the transition from nonmagnetic to antiferromagnetic behavior, and generally shows a gradual and continuous increase in local moments as

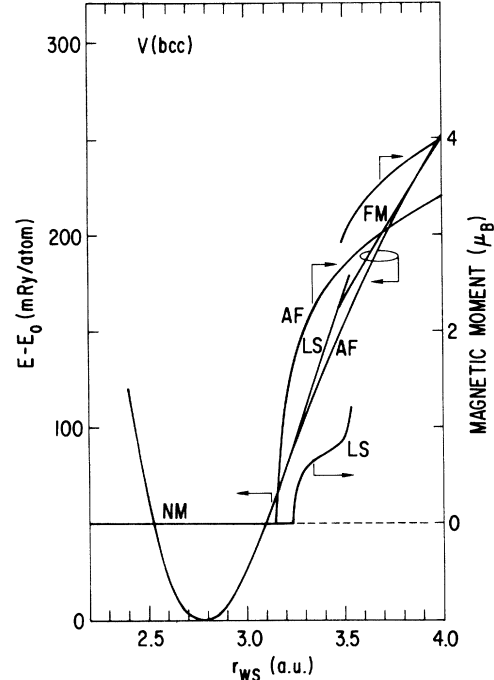


FIG. 1. Zero-field total energy and magnetic moment for bcc vanadium showing nonmagnetic (NM), low-spin (LS), ferromagnetic (FM), and antiferromagnetic (AF) branches. The reference energy  $E_0$  is the energy minimum for the nonmagnetic state.

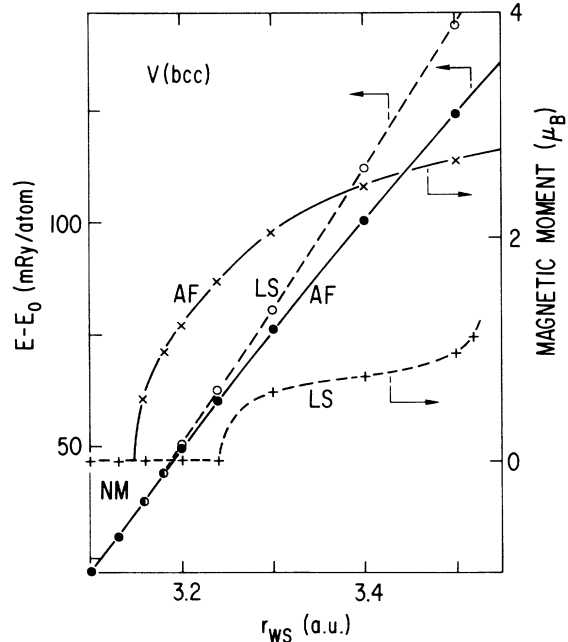


FIG. 2. High-resolution zero-field total energy and magnetic moment for vanadium showing details of the magnetovolume transitions. The calculated total-energy and magnetic-moment values for the one-atom bcc unit cell are indicated by open circles and + symbols, respectively; the values for the two-atom CsCl-type unit cell are indicated by solid circles and × symbols, respectively. Note that the antiferromagnetic solutions are energetically more favorable than the low-spin (LS) solutions and that the nonmagnetic-antiferromagnetic transition is second order.

the volume increases. In Fig. 3, we present our fixed-spin-moment results for this system. The calculated results in the range from  $r_{\text{WS}}=2.6$  to  $r_{\text{WS}}=3.0$  a.u. are shown on an expanded scale in Fig. 4. Note that the antiferromagnetic solutions are energetically more favored for  $r_{\text{WS}} > 2.72$  a.u., and that the transition from the nonmagnetic to the antiferromagnetic state is sharp and first order as indicated by the discontinuity in slope at the junction of the nonmagnetic and antiferromagnetic energy curves and the discontinuous jump of the antiferromagnetic local moments (AF). The equilibrium (zero-pressure) state for this constrained system is nonmagnetic with a lattice constant about 2% below the transition. This result is inconsistent with that of Chen *et al.*,<sup>10</sup> who find an antiferromagnetic equilibrium ground state.

A critical comparison of our fixed-spin-moment results for chromium with previous work shows important differences. In a two-atom cell conventional spin-polarized band calculation in which the local moments are constrained to be equal and opposite but with floating magnitudes, Kübler finds<sup>7</sup> the equilibrium solution to be antiferromagnetic at  $r_{\text{WS}} \approx 2.65$  a.u. with an energy  $\approx 4$  mRy below his nonmagnetic results. This work does not present the volume dependence of the energy and local moment, and does not show our first-order magnetovolume transition. We see from Fig. 4 that our fixed-spin-moment antiferromagnetic solutions do not extend below  $r_{\text{WS}}=2.72$  a.u., where the local moments are  $\pm 1.18\mu_B$  and where the energy is  $\approx 4$  mRy above our nonmagnetic equilibrium solution at  $r_{\text{WS}}=2.65$  a.u. Skriver<sup>8</sup> also used

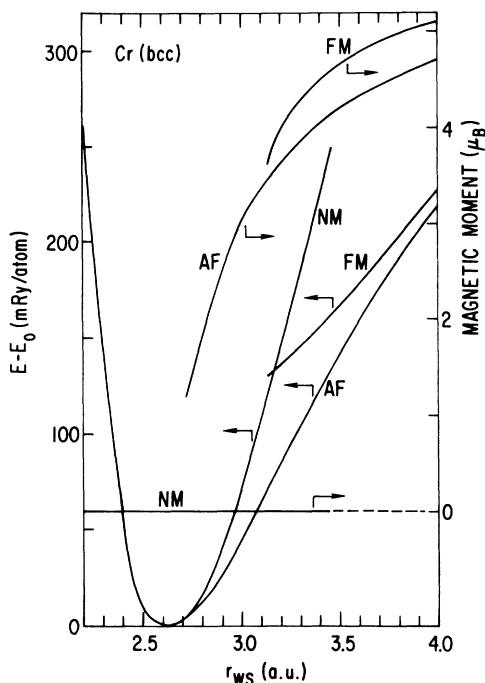


FIG. 3. Zero-field total energy and magnetic moment for bcc chromium showing nonmagnetic (NM), ferromagnetic (FM), and antiferromagnetic (AF) branches. The reference energy  $E_0$  is the energy minimum for the nonmagnetic state.

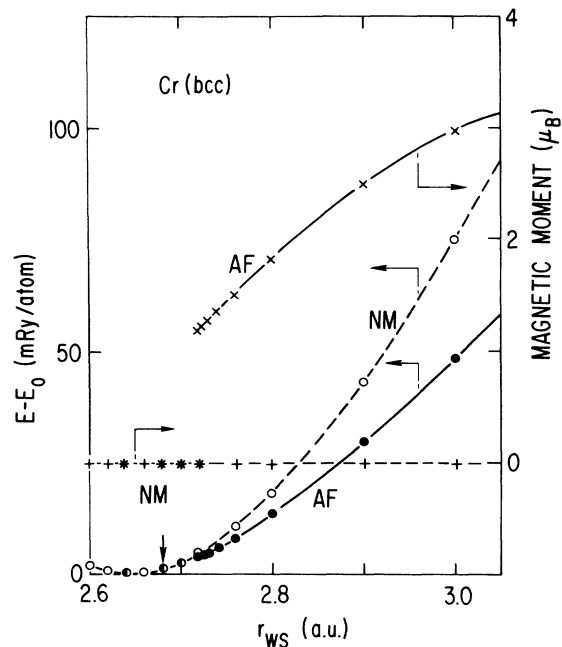


FIG. 4. High-resolution zero-field total energy and magnetic moment for chromium showing details of the magnetovolume transition. The calculated total-energy and magnetic-moment values for the one-atom bcc unit cell are indicated by open circles and + symbols, respectively; the values for the two-atom CsCl-type unit cell are indicated by solid circles and  $\times$  symbols, respectively. Note that the antiferromagnetic solutions are energetically more favorable than the nonmagnetic solutions at  $r_{\text{WS}} > \approx 2.72$  a.u., and that the nonmagnetic-antiferromagnetic transition is first order. The arrow at  $r_{\text{WS}}=2.68$  a.u. corresponds to the experimental lattice constant.

conventional spin-polarized band calculations with constrained equal and opposite local moments to study the volume dependence of the pressure ( $-dE/dV$ ) and local moments of bcc chromium in a two-atom cell constraint and found zero pressure at  $\approx 2.65$  a.u., in agreement with our results. He concludes that a lattice constant increase of a few percent would bring his calculated equilibrium properties into agreement with experiment. However, his work shows the local moments increasing smoothly from zero with increasing volume. The transition from nonmagnetic to antiferromagnetic behavior is therefore gradual and inconsistent with the critical behavior derived from our fixed-spin-moment calculations. In a recent two-atom cell bcc chromium calculation by Chen *et al.*,<sup>10</sup> the equilibrium volume was found at  $r_{\text{WS}} \approx 2.61$  a.u. The volume dependence of the local moments is in general agreement with Skriver's results and shows no evidence of our sharp first-order nonmagnetic-to-antiferromagnetic transition. We believe that the antiferromagnetic solutions below our transition volume ( $r_{\text{WS}}=2.72$ ) reported by Kübler, Skriver, and Chen *et al.* are unstable solutions and are a consequence of the equal and opposite local-moment constraint used.

Previous band calculations on bcc chromium have found higher values of the bulk modulus,  $B$  than experiment. Kübler,<sup>7</sup> Skriver,<sup>8</sup> and Chen *et al.*<sup>10</sup> find  $B=2130$ ,

2360, and 2650 kbar, respectively, where the experimental value<sup>21</sup> is  $\approx 1920$  kbar. Figure 4 shows that although the antiferromagnetic curve terminates above the minimum in the nonmagnetic curve, the former has a much lower curvature than the latter. As can be seen, the curvature, and the corresponding bulk modulus, is a function of  $r_{\text{WS}}$ . Our antiferromagnetic calculations yield  $B=1140$  kbar at  $r_{\text{WS}}=2.72$  a.u., but an extrapolation to the equilibrium radius of 2.65 a.u. gives  $B=1770$  kbar. The bulk modulus derived from our nonmagnetic curve at  $r_{\text{WS}}=2.65$  a.u. is 2540 kbar. Thus if an antiferromagnetic spin arrangement in a many-atom cell becomes the equilibrium state, as experiment indicates, it will probably yield a bulk modulus close to our extrapolated value of 1770 kbar, in reasonable agreement with experiment. The high values found in previous calculations probably arise from a failure to separate clearly the nonmagnetic and antiferromagnetic states, leading to a mixture that is influenced by the higher bulk modulus implied by the nonmagnetic states.

We note that band calculations on bcc chromium, including those reported in this work (except for Kübler's calculations, which do not show the volume dependence), do not give the observed local magnetic moment. However, from Fig. 4, an extrapolation of our local moments to  $r_{\text{WS}}=2.65$  a.u., yields reasonable agreement. Although Chen *et al.* conclude that their disagreement is due to a failure of the local-density approximation used in all of these total-energy band calculations, we suggest it may be due to the two-atom cell constraint as will be discussed below.

### III. DISCUSSION

All total-energy band calculations are subject to implied constraints such as volume, lattice type, moment, cell size (cell atom count), etc. In conventional non-spin-polarized calculations, the lattice type and volume are constrained to specific values by specifying the unit cell and the lattice parameter. In this case, the moment is implicitly constrained to be zero by the non-spin-polarized treatment. The self-consistent calculations determine the minimum energy for the system subject to the imposed constraints. By varying the volume constraint and finding the minimum in the resulting total-energy curve, we determine the equilibrium volume, or the solution that is stable with respect to volume variations (but that is still subject to all of the other constraints). Conventional spin-polarized calculations allow the moment (no longer constrained to be zero) to float. The self-consistent calculations then determine the moment required to minimize the total energy. In cases where there are two (or more) local minima at different moment values, conventional spin-polarized calculations can converge only with difficulty, or can "accidentally" converge on either solution.

Our fixed-spin-moment procedure was developed primarily to avoid the above mentioned convergence difficulties and the accidental convergence in systems with multiple solutions. In our case, the total moment is no longer allowed to float; it is fixed or constrained to a

specific value, and the calculations now determine the minimum total energy under this moment constraint. By varying this constraint, we now determine the entire  $E(M)$  curve and identify all the local minima as solutions that are stable with respect to moment variations.

In order to find possible antiferromagnetic solutions, we consider a unit cell that can accommodate an antiparallel spin arrangement, and study antiferromagnetism in bcc metallic elements by considering a two-atom CsCl-type cell. This is the first step in a variation of the size of the unit cell. Since the two atoms are allowed to be inequivalent, this variation can lead to new solutions. In fact, increasing the size (i.e., the atom count) of the unit cell can have a number of consequences. For example, a two-atom cell can yield a minimum-energy solution that is the same as that of a one-atom cell, in which case the one-atom cell solution is stable or metastable relative to the change from a one-atom to two-atom cell. However the one-atom solution can have an energy maximum with respect to a two-atom solution and hence be unstable. In the two-atom cell case, a minimum at  $M=0$  with  $m_a = m_b = 0$  corresponds to a stable nonmagnetic state, a minimum at  $M=0$  with  $m_a = -m_b \neq 0$  corresponds to a stable antiferromagnetic state, while a maximum at  $M=0$  corresponds to an unstable nonmagnetic or antiferromagnetic state. In this latter case,  $E(M)$  will display a minimum at a finite  $M$  value corresponding to a stable ferromagnetic or ferrimagnetic state depending upon whether  $m_a = m_b$  or  $m_a \neq m_b$ , respectively.

We illustrate these general comments on the stability of solutions with three specific examples of constraint variation. In Fig. 5 we show a set of solutions for vanadium constrained to a one-atom bcc unit cell and to a two-

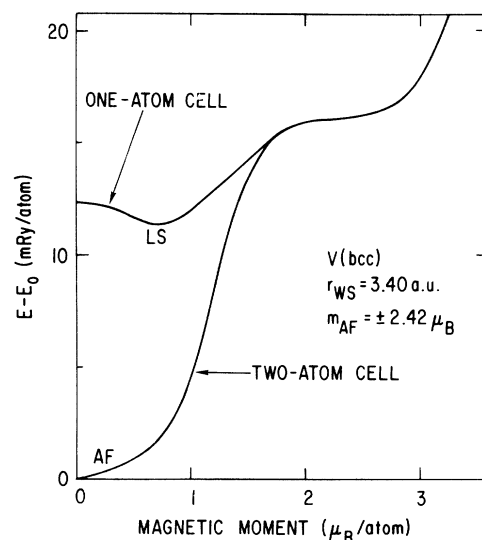


FIG. 5. Energy vs moment curves for bcc vanadium at  $r_{\text{WS}}=3.40$  a.u., with one-atom cell and two-atom cell constraints. The "stable" low-spin (LS) one-atom cell solution is metastable when a two-atom cell is considered. The local antiferromagnetic moments at  $M=0$  for the two-atom cell,  $m_{\text{AF}}$ , are  $\pm 2.42\mu_B$ . The decrease in slope at  $M \approx 2\mu_B$  in both calculations indicates the precursor of a high-spin ferromagnetic solution.

atom CsCl unit cell at a volume corresponding to  $r_{\text{WS}} = 3.40$  a.u. as a function of the constrained moment  $M$ . The one-atom cell solutions show the local energy minima at  $\approx 0.7\mu_B$ , which we have previously identified<sup>2,3</sup> as a low-spin (LS) solution. The two-atom cell calculation displays a local minimum at  $M=0$  with  $\approx 11$  mRy lower energy corresponding to an antiferromagnetic solution with local moments of  $\approx \pm 2.42\mu_B$ . The two curves merge<sup>22</sup> smoothly at  $M \approx 1.8\mu_B$  and show evidence of the precursor of the high-spin ferromagnetic solution by the decrease in slope at  $\approx 2\mu_B$ . In Fig. 6 we show similar behavior for chromium at  $r_{\text{WS}} = 3.30$  a.u., except that the one-atom cell solutions now show two local energy minima at  $M=0$  and at  $M \approx 4.25\mu_B$  that can be identified as the “metastable” and “stable” solutions labeled NM and FM. However, the two-atom cell calculation displays a lower-energy minimum labeled AF that corresponds to an antiferromagnetic solution at  $M=0$  with local moments of  $\pm 3.86\mu_B$ . The local moments become equal and parallel when the curve merges<sup>22</sup> with the one-atom cell curve. Thus, by removing the one-atom cell constraint, we find the original “stable” FM solution is, in fact, metastable with respect to the antiferromagnetic solution. Conventional non-spin-polarized calculations would only find our NM solution, conventional spin-polarized calculations would only find our FM solution, and conventional antiferromagnetic calculations (two-atom cell) would only yield our AF solution. Our fixed-spin-moment procedure displays all solutions and provides information on their stability by introducing a controlled magnetic-moment constraint.

In Fig. 7 we give another example of constraint variation that shows different behavior as  $M$  is varied. Here we show the results for iron constrained to a one-atom

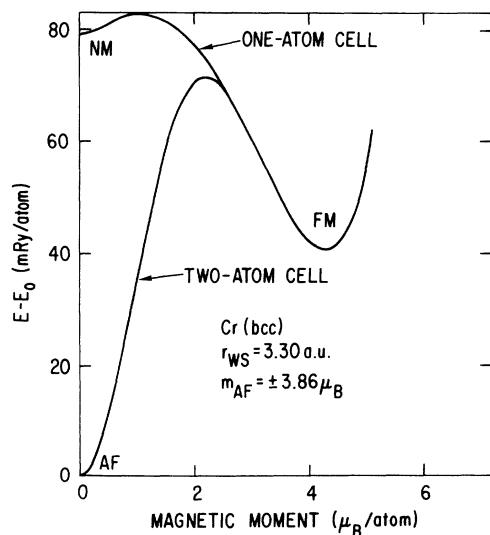


FIG. 6. Energy vs moment curves for bcc chromium at  $r_{\text{WS}} = 3.30$  a.u., with one-atom cell and two-atom cell constraints. The “stable” nonmagnetic (NM) and ferromagnetic (FM) one-atom cell solutions are metastable when a two-atom cell is considered. The local antiferromagnetic moments at  $M=0$  for the two-atom cell,  $m_{\text{AF}}$ , are  $\pm 3.86\mu_B$ .

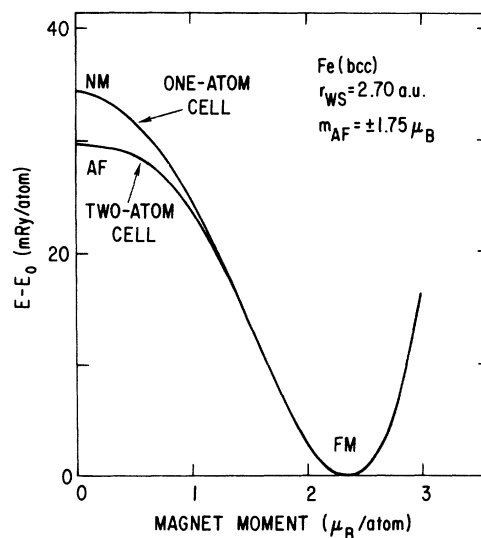


FIG. 7. Energy vs moment curves for bcc iron  $r_{\text{WS}} = 2.70$  a.u., with one-atom cell and two-atom cell constraints. The nonmagnetic (NM) one-atom cell and antiferromagnetic (AF) two-atom cell solutions are unstable. The local antiferromagnetic moments at  $M=0$  for the unstable two-atom cell AF solution,  $m_{\text{AF}}$ , are  $\pm 1.75\mu_B$ .

bcc unit cell and to a two-atom CsCl unit cell. The minimum in the one-atom cell curve shows the existence of the stable ferromagnetic solution at  $M \approx 2.34\mu_B$  labeled FM. The maximum at  $M=0$  in this same curve identifies an unstable nonmagnetic solution labeled NM. Note that the two-atom cell curve at  $M=0$  has a local maximum with a lower energy and that this curve merges smoothly with the one-atom cell curve. The two-atom cell curve exhibits an unstable antiferromagnetic solution with local moments of  $\approx \pm 1.75\mu_B$  labeled AF. At the point where the two curves merge,<sup>22</sup> the local moments in the two-atom cell become equal and parallel and have the same values as the one-atom cell. This unstable antiferromagnetic solution was also found by Kübler,<sup>14</sup> who considered it to be metastable.

The various solutions described above change with changes in the volume constraint. Nonmagnetic solutions generally first become metastable and then become unstable with increasing volume. This behavior is illustrated in Fig. 3, where we show that for bcc chromium the nonmagnetic solutions terminate at  $r_{\text{WS}} \approx 3.44$  a.u., while the ferromagnetic solutions begin at  $r_{\text{WS}} \approx 3.13$  a.u. In the one-atom cell calculation the nonmagnetic solutions are stable up to 3.13 a.u., metastable from 3.13 to 3.44 a.u., and unstable above 3.44 a.u. The ferromagnetic one-atom cell solutions are stable above  $r_{\text{WS}} \approx 3.13$  a.u. When the one-atom cell constraint is relaxed by considering a two-atom cell, antiferromagnetic solutions appear with lower energies for  $r_{\text{WS}} > \approx 2.72$  a.u. The one-atom cell NM solutions for  $r_{\text{WS}} > \approx 2.72$  a.u. and the one-atom cell FM solutions above  $r_{\text{WS}} \approx 3.13$  are now identified as metastable. The first-order transition from nonmagnetic-to-ferromagnetic behavior implied by the one-atom cell constraint is therefore a transition between

metastable states.

Notice that the unusual *first-order* transition from nonmagnetic-to-antiferromagnetic behavior for bcc chromium at  $r_{\text{WS}} \approx 2.72$  a.u. suggests that lower-energy solutions and different transitions may exist by further reducing the cell size constraint from a two-atom cell to a many-atom cell, just as the first-order transition from nonmagnetic-to-ferromagnetic behavior discussed above was altered by going from a one-atom cell to a two-atom cell constraint. A many-atom cell with elaborate moment configurations may even describe the equilibrium state of the system, i.e., the solution that is stable with respect to the volume constraint. We note that the two-atom cell antiferromagnetic branch begins at a  $r_{\text{WS}}$  value that is only 2% above the value corresponding to the equilibrium nonmagnetic volume. The incommensurate spin-density wave found experimentally is actually close to a 20-atom cell description. A similar reduction of energy in a many-atom cell may plausibly be expected in bcc manganese, where we found<sup>12</sup> evidence, based on two-atom cell calculations, of a first-order transition from nonmagnetic-to-ferrimagnetic solutions; a many-atom cell is in fact found experimentally.

In all of the fixed-spin-moment calculations described in the present work, we have implicitly constrained the local moments to be colinear. As discussed above, the two-atom cell antiferromagnetic solutions shown explicitly in Figs. 5–7 only exist at  $M=0$ . A nonzero  $M$  in our calculations still *requires* antiparallel or parallel (colinear) local moments. Deviation from the antiferromagnetic  $M=0$  solution involves local moments of unequal magni-

tude. However, Kübler *et al.*<sup>23</sup> have shown that this colinear moment constraint can also be removed and that solutions involving tetrahedral and triangular spin arrangements can be found.

Finally, we mention that still another constraint that can be varied is the constraint to a cubic cell. For example, by allowing for tetragonal distortions of the fcc (CuAu) two-atom cell, more favorable lower-energy antiferromagnetic solutions can be found. Oguchi and Freeman<sup>9</sup> find such a distortion for fcc manganese. Many-atom magnetic cells of a bcc or fcc lattice may, in addition to elaborate moment configurations, also be expected to show relaxations of atomic positions from the basic structure. Thus the systematic variation of constraints in total-energy calculations can lead to a great variety of stable and metastable structures even in the elements.

In conclusion, unlike Chen *et al.*,<sup>10</sup> we find no reason to question the accuracy of the local-spin-density approximation in calculating lattice constants, magnetic moments, and bulk moduli of both ferromagnetic and antiferromagnetic states in these systems. We survey the occurrence of ferromagnetism and antiferromagnetism in all of the 3d transition metals and observe that antiferromagnetism seems to occur only when a transition to ferromagnetic behavior is first order. Total-energy calculations over selected but reasonable volume ranges yield no evidence for stable or metastable antiferromagnetic solutions for scandium, titanium, iron, cobalt and nickel in the bcc form, nor for scandium, titanium, vanadium, chromium, and nickel in the fcc form.

<sup>1</sup>O. K. Andersen, J. Madsen, U. K. Poulsen, O. Jepsen, and J. Kollar, *Physica B* **86-88**, 249 (1977).

<sup>2</sup>V. L. Moruzzi, P. M. Marcus, K. Schwarz, and P. Mohn, *Phys. Rev. B* **34**, 1784 (1986); V. L. Moruzzi, P. M. Marcus and P. C. Pattnaik, *ibid.* **37**, 8003 (1988); V. L. Moruzzi and P. M. Marcus, *ibid.* **38**, 1613 (1988); V. L. Moruzzi and P. M. Marcus, *J. Appl. Phys.* **64**, 5598 (1988).

<sup>3</sup>V. L. Moruzzi, *Phys. Rev. Lett.* **57**, 2211 (1986).

<sup>4</sup>Y. Endoh and Y. Ishikawa, *J. Phys. Soc. Jpn.* **30**, 1614 (1971).

<sup>5</sup>S. Asano and J. Yamashita, *J. Phys. Soc. Jpn.* **31**, 1000 (1971).

<sup>6</sup>J. Kübler, *J. Magn. Magn. Mater.* **20**, 107 (1980).

<sup>7</sup>J. Kübler, *J. Magn. Magn. Mater.* **20**, 277 (1980).

<sup>8</sup>H. L. Skriver, *J. Phys. F* **11**, 97 (1981).

<sup>9</sup>T. Oguchi and A. J. Freeman, *J. Magn. Magn. Mater.* **46**, L1 (1984).

<sup>10</sup>J. Chen, D. Singh, and H. Krakauer, *Phys. Rev. B* **38**, 12 834 (1988).

<sup>11</sup>V. L. Moruzzi, P. M. Marcus, and J. Kübler, *Phys. Rev. B* **39**, 6957 (1989).

<sup>12</sup>V. L. Moruzzi and P. M. Marcus, *Solid State Commun.* **71**, 203 (1989).

<sup>13</sup>H. Duschaneck, P. Mohn, and K. Schwarz, *Physica B* **161**, 139 (1989).

<sup>14</sup>J. Kübler, *Phys. Lett.* **81A**, 81 (1981).

<sup>15</sup>F. J. Pinski, J. Staunton, B. L. Gyorffy, D. D. Johnson, and G. M. Stocks, *Phys. Rev. Lett.* **56**, 2096 (1986).

<sup>16</sup>A. R. Williams, V. L. Moruzzi, J. Kübler, and K. Schwarz,

*Bull. Am. Phys. Soc.* **29**, 278 (1984).

<sup>17</sup>An alternative fixed-spin-moment procedure (see, e.g., Refs. 11 and 13), which yields similar results, constrains the local moments to be equal and opposite with a fixed magnitude  $m$ . In this case, a minimum in  $E(m)$  at  $m=0$  implies a stable nonmagnetic solution, while a maximum at  $m=0$  implies an unstable nonmagnetic solution. In this latter case,  $E(m)$  will have a minimum at a finite  $m$  value corresponding to a stable antiferromagnetic solution. This alternative procedure excludes ferromagnetic solutions.

<sup>18</sup>A. R. Williams, J. Kübler, and C. D. Gelatt, Jr., *Phys. Rev. B* **19**, 6094 (1979).

<sup>19</sup>U. von Barth and L. Hedin, *J. Phys. C* **5**, 1692 (1972); J. F. Janak, *Solid State Commun.* **25**, 53 (1978).

<sup>20</sup>T. M. Hattox, J. B. Conklin, Jr., J. C. Slater, and S. B. Trickey, *J. Phys. Chem. Solids* **34**, 1627 (1973).

<sup>21</sup>W. C. Muir, J. M. Perz, and E. Fawcett, *J. Phys. F* **17**, 2431 (1987). We extrapolate the elastic moduli,  $C_{11}$  and  $C_{12}$ , for the single- $Q$  antiferromagnetic phase to zero temperature to find the experimental bulk modulus. See also, D. I. Bolef and J. de Klerk, *Phys. Rev.* **129**, 1063 (1963).

<sup>22</sup>In some cases (see, e.g., Ref. 11), the two-atom cell  $E(M)$  curves cross the one-atom cell curves instead of merging smoothly as shown in Figs. 5–7.

<sup>23</sup>J. Kübler, K.-H. Höck, J. Stricht, and A. R. Williams, *J. Appl. Phys.* **63**, 3482 (1988); *J. Phys. F* **18**, 169 (1988).